Arabian Journal of Chemistry (2020) **13**, 8723–8733

King Saud University

Arabian Journal of Chemistry

www.ksu.edu.sa
www.sciencedirect.com

ORIGINAL ARTICLE

Synthesis of three-dimensional hydrogels based on poly(glycidyl methacrylate-*alt*-maleic anhydride): Characterization and study of furosemide drug release

Kobra Akbari, Peyman Najafi Moghadam *, Mohammad Behrouzi, Amir Reza Fareghi

Department of Organic Chemistry, Faculty of Chemistry, Urmia University, Urmia, Iran

Received 27 June 2020; accepted 1 October 2020
Available online 15 October 2020

KEYWORDS

Hydrogel;
Poly(glycidyl methacrylate-alt-maleic anhydride);
Furosemide;
In vitro release

Abstract In the present work, three-dimensional drug carriers were synthesized via chemical modification of poly (glycidyl methacrylate-*alt*-maleic anhydride) P(GMA-alt-MA) by isopropylamine (IPA) and ethylenediamine (EDA) with different molar ratios. Then furosemide drug (FR) was loaded on the hydrogels and studied for its slow release in phosphate-buffered saline (PBS) solution (pH = 7.41) at 37 °C. According to the obtained results, the sample with the lowest amount of crosslinking agent (Sample A) showed the highest swelling ratio in comparison to the others. By increasing the rigidity of carrier in the result of increasing the crosslinker density, the amount of the released drug was decreased. However, the release rate for all of samples (slope of the profiles) were rather similar. All the synthesized carriers have shown pH dependent properties and the maximum release rate was shown in basic pH. Also, the drug release experiments in different temperatures showed almost thermal sensitivity properties for synthesized carriers and release rate become faster by increasing the medium temperature. The FT-IR, TGA, and FE-SEM analyses were carried out for characterization of prepared samples and the swelling behavior of prepared hydrogels were measured too. Investigation of the release data with different mathematical models showed the highest adaption with the Higuchi model for all samples.

* Corresponding author.
E-mail addresses: p.najafi@urmia.ac.ir, p_najafi27@yahoo.com (P. N. Moghadam).
Peer review under responsibility of King Saud University.

ELSEVIER Production and hosting by Elsevier

1. Introduction

Hydrogels are referred to a group of materials with three-dimensional hydrophilic networks that are cross-linked with covalent bonds, hydrogen bonds, or Van der Waals' forces and are able to absorb and preserve water or biological fluids (Ahmed, 2015; Kashyap et al., 2005; Maia et al., 2009).

https://doi.org/10.1016/j.arabjc.2020.10.003
1878-5352

Hydrogels can be physically or chemically networked, and their porous structure can be controlled by network density. Due to their biocompatibility, high water content, and physiological resemblance to the extracellular matrix (Hoare and Kohane, 2008), hydrogels have many opportunities for applications in medical fields, including the fabrication of contact lenses (Wichterle and LIM, 1960), sanitation products (Omidian et al., 2005), tissue engineering scaffolds (Chen et al., 2000), wound dressings (Cartmell et al., 1996), and drug delivery systems (Ciolino et al., 2013; Mano et al., 2002; Vashist et al., 2014). The hydrogels have been developed as stimuli-responsive materials, which can undergo sudden volume changes in response to small changes in their environmental factors, including the temperature, pH, and ionic strength. The stimuli-responsive polymers play an important role in the development of novel smart hydrogels and their unrivaled characteristics are of interest in drug delivery, cell encapsulation, and tissue engineering (Lee and Mooney, 2001).

The use of hydrogels for therapeutic applications began in the 1960s when Lim and Wichterle synthesized poly (2-hydroxyethyl methacrylate) (PHEMA) (Wichterle and LIM, 1960). In designed systems with diffusion-controlled drug delivery which are represented by repository or matrix devices, the drug releases were done by propagation through the hydrogel mesh or pores. The existing gradient between the hydrogel and the release medium permits the diffusion of the drug (Bierbrauer, 2005). Currently, due to unique properties as drug carrier in drug delivery systems, hydrogels have wide variety of applications in slow release processes. Possibility of prolonged release, which leads to maintain a local concentration of an active medicinal ingredient over a long period of time, is one of the important advantages of hydrogels in the recent drug delivery systems (Ciolino et al., 2013). Furosemide, systematically named as 5-(aminosulfonyl)-4-chloro-2-([2 furanylmethyl] amino) benzoic acid, is a powerful drug that induces a potent diuresis whose action is correlated with blocking reabsorption of ions in the ascending limb of Henle's loop (long U-shaped portion of the tubule that conducts urine) and loss of sodium, potassium and chloride into the urine (Limmer et al., 2015). This medication is used for the therapy of congestive heart failure (Owen et al., 2015), chronic renal failure (Cheng et al., 2014), and cirrhosis of the liver (Franz et al., 2013). But it is used as a common therapy for treatment of hypertension (Pourzitaki et al., 2016; Vigil-De Gracia et al., 2014). Alongside serious side effects of Furosemide as electrolyte abnormalities and hearing loss, the most common side effect is rapid decrease in blood pressure (Lin et al., 2016). So, the controlled usage of this drug is required. In recent years, many researches have been conducted on Furosemide slow-release systems. One of these efforts is the synthesized Furosemide-loaded alginate microspheres with ionic cross-linking technique using $CaCl_2$, $Al_2(SO_4)_3$ and $BaCl_2$. The sodium alginate concentration, kind of cross-linking agent and drying conditions influenced the amount and time of release of furosemide drug (Das and Senapati, 2008).

In another work a gastroretentive mucoadhesive dosage form of furosemide for a controlled release system was designed by Vavia and et al. It contains a drug loaded polymeric film prepared from a bilayer of immediate and controlled release layers folded into a hard gelatin capsule (Darandale and Vavia, 2012).

Post-polymerisation modification of poly (glycidyl methacrylate) through the nucleophilic ring opening reactions of the pendent epoxide groups was carried out for the installation of a variety of functionalities onto the reactive scaffold by ezzah and et al. (Muzammil et al., 2017). In that work presented an opportunity to modify one scaffold in a one-pot or sequential manner with different nucleophiles to generate multiply functionalized polymers.

R.X. Zhuo and et al. reported the synthesis of shell cross-linked thermoresponsive hybrid micelles consisting of a cross-linked thermoresponsive hybrid hydrophilic shell and a hydrophobic core domain from poly (N-isopropylacrylamide-co-3-(trimethoxysilyl)propyl methacrylate)-b-polymethyl methacrylate amphiphilic block copolymers. The synthesized micelles have a much higher stability due to the presence of the cross-linked silica network, which results in a much improved entrapment efficiency as well as a rather retarded drug release (Zhuo et al., 2008).

Soluble poly (N-isopropylacrylamide-*co*-3-(trimethoxysilyl) propyl methacrylate) copolymers is synthesized by Ivan and et al. for obtaining a variety of novel smart thermoresponsive complex and hybrid materials (Osvath et al., 2017).

In recent years, the copolymers containing the GMA have attracted much interest due to the presence of the epoxide groups, which can allow large number of chemical modifications on the copolymer as like as anhydride group (Sinirlioglu et al., 2015; Trachtova et al., 2015).

In the present investigation, poly (glycidyl methacrylate-*alt*-maleic anhydride) P (GMA-alt-MA) copolymer was synthesized via free radical polymerization (Hasanzadeh et al., 2016; Shohraty et al., 2018), and used as the backbone polymer for further modification. Then isopropylamine (IPA) and ethylenediamine (EDA) were used as modifying and crosslinking agents respectively in different molar ratios (90:10, 80:20, and 70:30 for IPA to EDA, according to the mole of the copolymer active sites) to prepare the final carriers. Furosemide drug (FR) was then loaded on each of the carriers and the slow release studies were carried out. The release process was done in pH = 7.41 phosphate-buffered saline (PBS) solution at 37 °C, which was simulated the normal body pH and temperature.

2. Experimental

2.1. Materials

Glycidyl methacrylate (GMA) (>98% Daejung) was distilled by vacuum distillation before use. Maleic anhydride (MA) (>99% Merck), isopropylamine (IPA) (Merck), ethylenediamine (EDA) (≥99% Merck) and tetrahydrofuran (THF) (≥99% Daejung) were used without further purification. α,α′-Azoisobutyronitrile (AIBN) (≥98% Merck) was recrystallized from hot methanol (50 °C) before use. Furosemide (FR, MW = 330.74, log $P_{o/w}$ = 2.29, 20 mg/2 mL vials, 10,000 ppm solutions in deionized water) was donated by Alborz Darou Pharmaceutical Co., Qazvin - Iran, and used in diluted form without any alterations. The chemical structure of the drug is depicted in Fig. 1. Phosphate buffered saline (PBS) solution (0.1 M, pH = 7.41) was prepared by complete dissolving of NaCl (8.0 g), KCl (2.0 g), Na_2PO_4 (2.0 g) and, KH_2PO_4 (0.24 g) in deionized water (800 mL). The desired

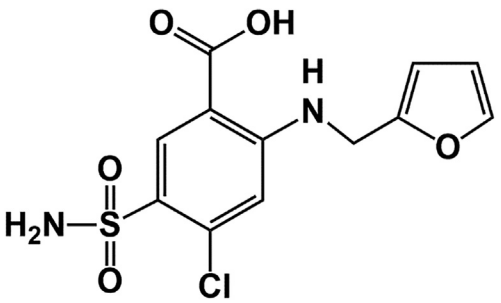

Fig. 1 The chemical structure of Furosemide drug.

pH was adjusted by adding HCl or NaOH solution and the final volume of solution was adjusted in 1000 mL in volumetric flask by adding deionized water.

2.2. Apparatus

The FT-IR and UV–Vis. spectra were recorded by Thermo Nicolet NEXUS 670 Fourier transform infrared spectrophotometer (USA) and Agilent 8453 Diode Array UV–Vis. spectrophotometer (USA), respectively. The ^{1}H NMR measurement was performed with a BRUKER spectrometer in CDCl3 (Lambda 300 MHz). The thermogravimetric analysis (TGA) was studied by STA PT1000 TG-DSC (STA Simultaneous Thermal Analysis) thermogravimetric analyzer (Linseis Thermal Analysis, Germany) at a heating rate of 10 °C/min under N_2 atmosphere. The field-emission scanning electron microscopy (FE-SEM) images were obtained from MIRA3 (TE-SCAN-UK, Ltd).

2.3. Synthesis of poly (glycidyl methacrylate-alt-maleic anhydride) P (GMA-alt-MA)

In a 100 mL two-necked round-bottom flask equipped with a magnetic stirrer, a reflux condenser and gas inlet and outlet, MA (2.00 g, 20.40 mmol), dry THF (60 mL), and GMA (2.90 g, 20.40 mmol) were added respectively. The content of the flask was deoxygenated by inert gas (Argon) using a capillary tube for 20 min at room temperature to remove any dissolved oxygen that could inhibit the reaction, followed by

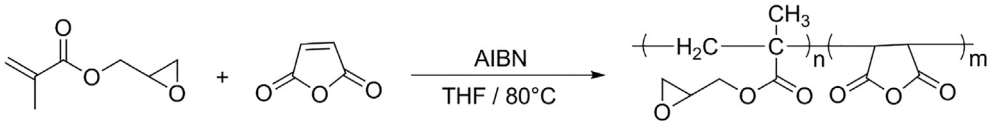

Scheme 1 The schematic representation of the P(GMA-alt-MA) synthesis.

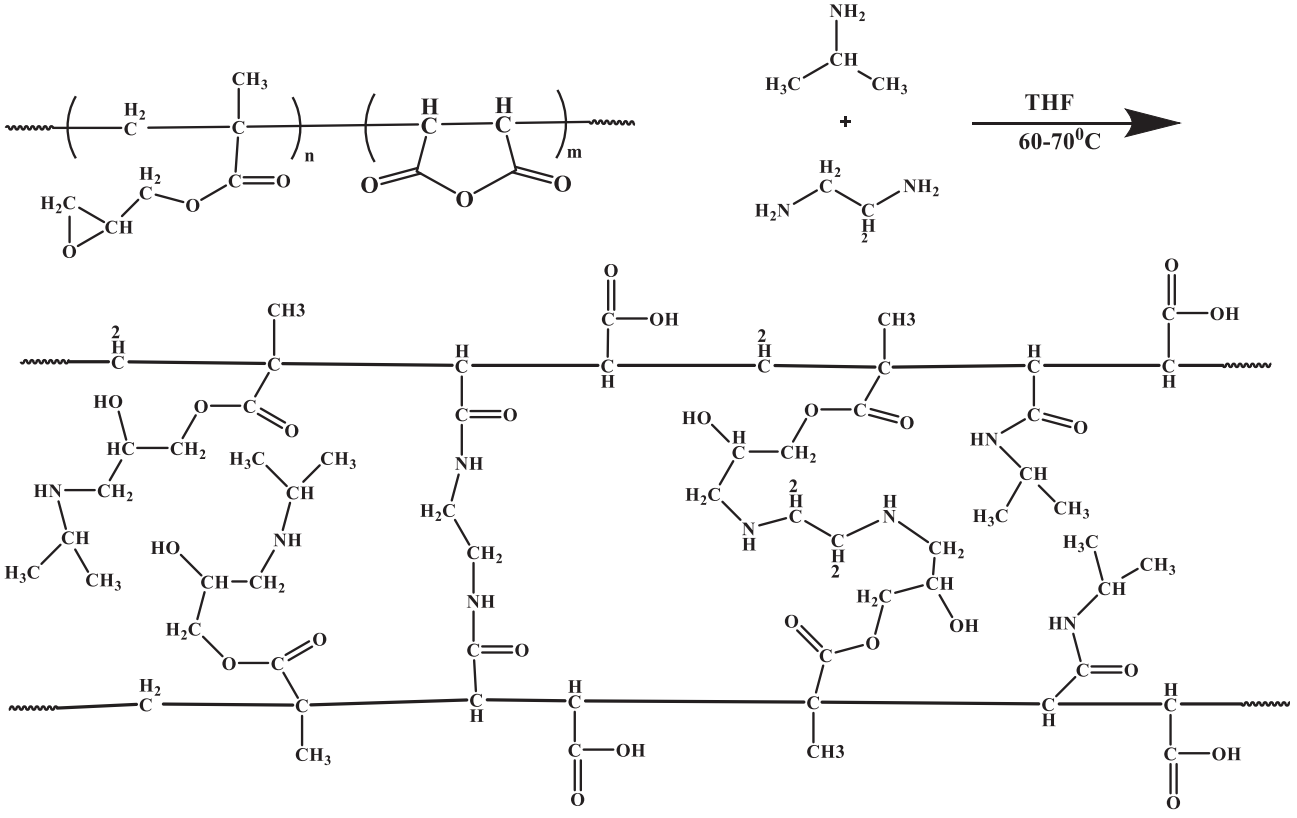

Scheme 2 Synthesis of the P(GMA-alt-MA) network by IPA and EDA.

the addition of AIBN (0.013 g, 8.00 mmol) was carried out. The whole system was kept under inert atmosphere and stirred overnight at 80 °C. The final product was precipitated in n-hexane (150 mL). The precipitate was filtered, washed several times with n-hexane and dried at room temperature. In order to prevent self-crosslinking (Hasanzadeh et al., 2016) the product was used immediately after drying.

2.4. Modification of P(GMA-alt-MA) by IPA and EDA with various molar ratios

In a 100 mL round-bottom flask equipped with a magnetic stirrer and a reflux condenser, the P(GMA-alt-MA) (750 mg, 6.64 mmol of active groups) and dry THF (80 mL) were added and stirred at room temperature to complete dissolution. Separately, the IPA and EDA with molar ratios of 90:10, 80:20, or 70:30 for IPA to EDA, according to the mole of the copolymer active sites were dissolved in dry THF (5 mL) and added to the flask containing P(GMA-alt-MA) solution. The reaction mixture was stirred at 60–70 °C for 24 h. After that, the content of the flask was cooled in the ice bath and the precipitate was separated and washed several times with 1 M NaCl followed by methanol to remove excess ethylenediamine and NaCl respectively. The final precipitate was dried at 70 °C under vacuum for 24 h. The samples were named as A, B, and C according to the ratios 90:10, 80:20, and 70:30, respectively.

2.5. Swelling studies

The synthesized polymers were studied for their swelling behavior in PBS solution (pH = 7.41). For this purpose, 10 mg of each sample was weighed precisely and placed into pre-weighed wet tea bag. Then the tea bag was plunged in 200 mL of the buffer solution. At specific time intervals, the tea bag was picked up from the solution and re-weighed until reaching to a constant weigh, which is defined as equilibrium

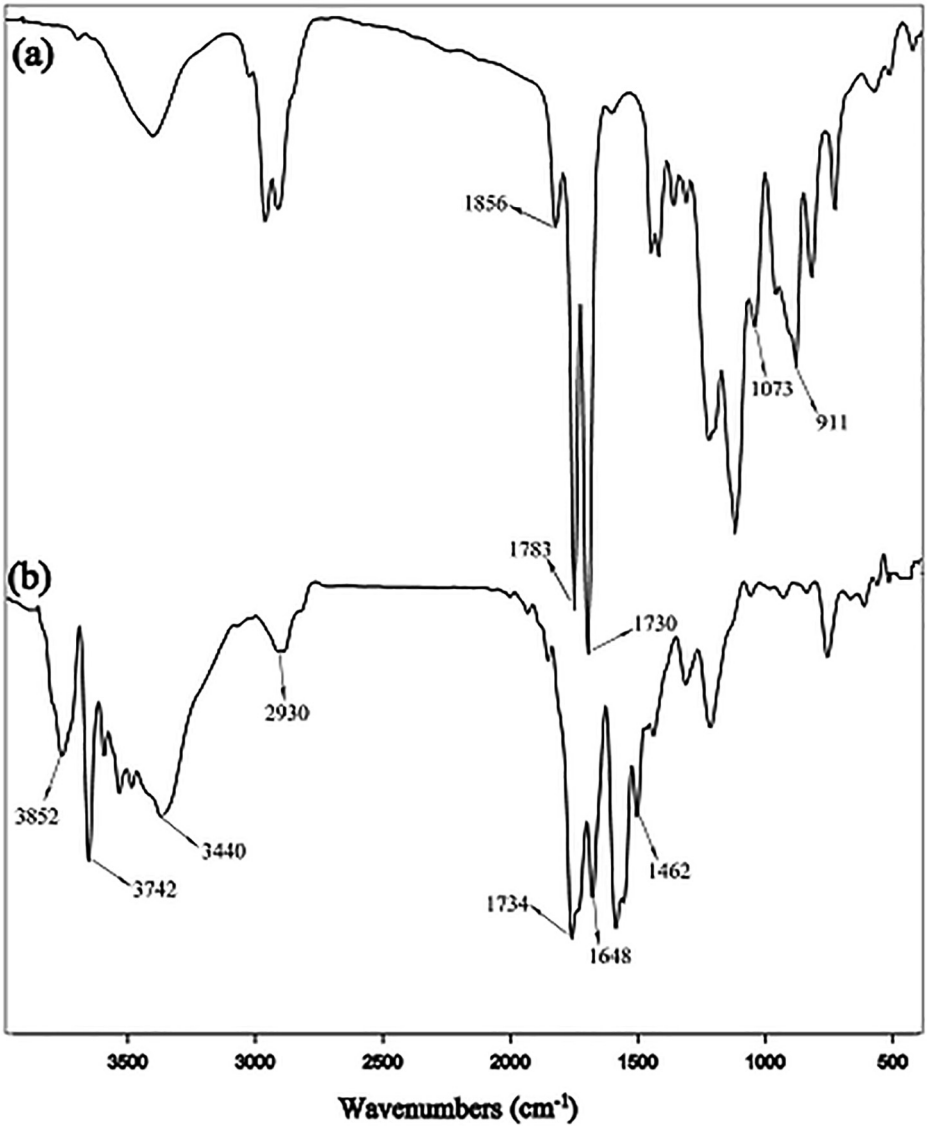

Fig. 2 The FT-IR spectra of P(GMA-alt-MA) (a) and Sample A (b).

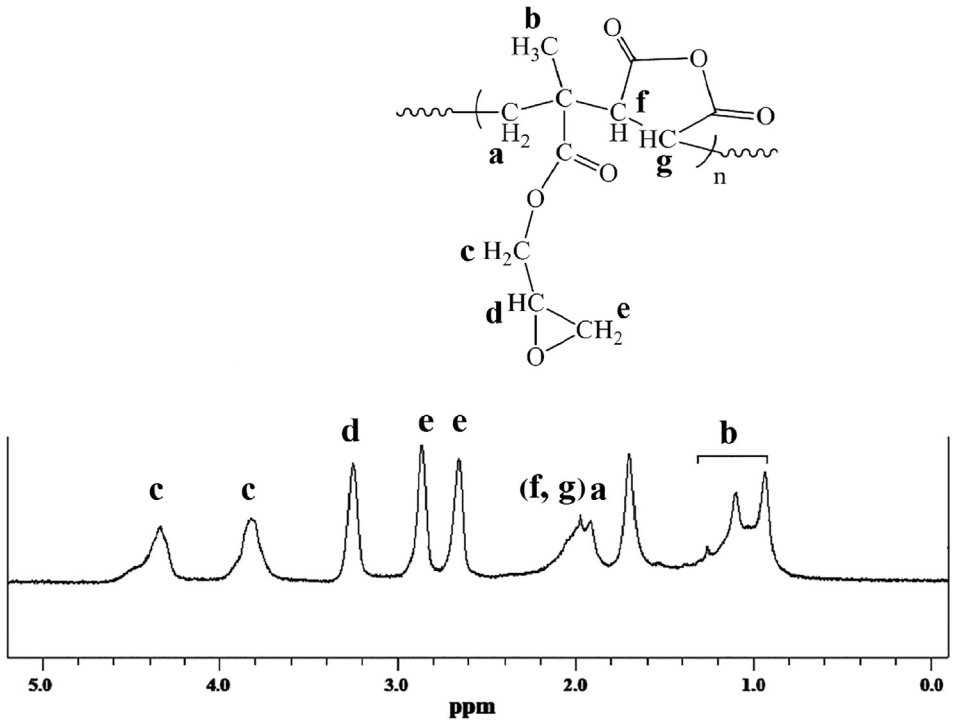

Fig. 3 The H-NMR spectrum of P(GMA-alt-MA) copolymer in $CDCl_3$.

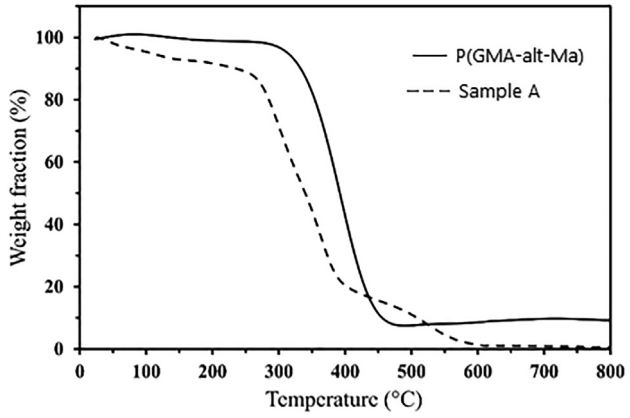

Fig. 4 The TGA thermograms of the P(GMA-alt-MA) and sample A.

swelling ratio (ESR). The ESR was calculated for the samples A, B and C according to the following equation and the obtained data were 9.5, 7.6 and 6.8 respectively.

$$ESR = \frac{(W_{eq} - W_1 - W_0)}{W_1}$$

Where the W_{eq}, W_1 and W_0 represent, wet tea bag at the specified time, the weight of dry polymer, and the weight of empty wet tea bag respectively.

2.6. Drug loading and in vitro release studies

The loading process was carried out for each of the carriers via immersion procedure. For this purpose, 4 mL of the 10,000 ppm FR solution was poured into separate falcon conical centrifuge tubes. Then a precisely weighed amount of each sample was added into the tube and shaken slowly for 72 h in the dark medium at room temperature to obtaining the complete adsorption of the drug. The loaded polymer was then collected via centrifugation and for removing any surface-adhered drug it was rinsed fast with distilled water then dried at room temperature. To calculate the loading capacity (LC), the supernatant after loading was analyzed for the remaining amount of the drug. In this case, the subtraction of the remaining amount from the initial amount of the drug represents the loaded drug on the carrier (the probable rinsed drug in final rinsing process was ignored). Therefore, the loading capacity percentage (LC %) was calculated using the equation below:

$$LC\% = \frac{W}{W'} \times 100$$

Where the W is the net weight of the drug and W' is the weight of the dry polymer before loading. The loading capacity percentage for the samples A, B and C is 18.18, 9.51 and 8.76, respectively.

To study the in-vitro release process, 20 mg of the loaded polymer was introduced into a dialysis tube and immersed in a vial containing 50 mL of pH = 7.41 PBS solution placed in a thermostatic bath adjusted at 37 °C without stirring. At specific time intervals, the supernatant was analyzed with UV–Vis spectrophotometer at 330 nm. The release diagram of the drug for each of the loaded polymers was drawn in the form of cumulative drug release percentage as a function of time (Fig. 6). The same procedure was repeated in pH = 3 and 9. Also, the release studies in different pH were carried out in 45 °C

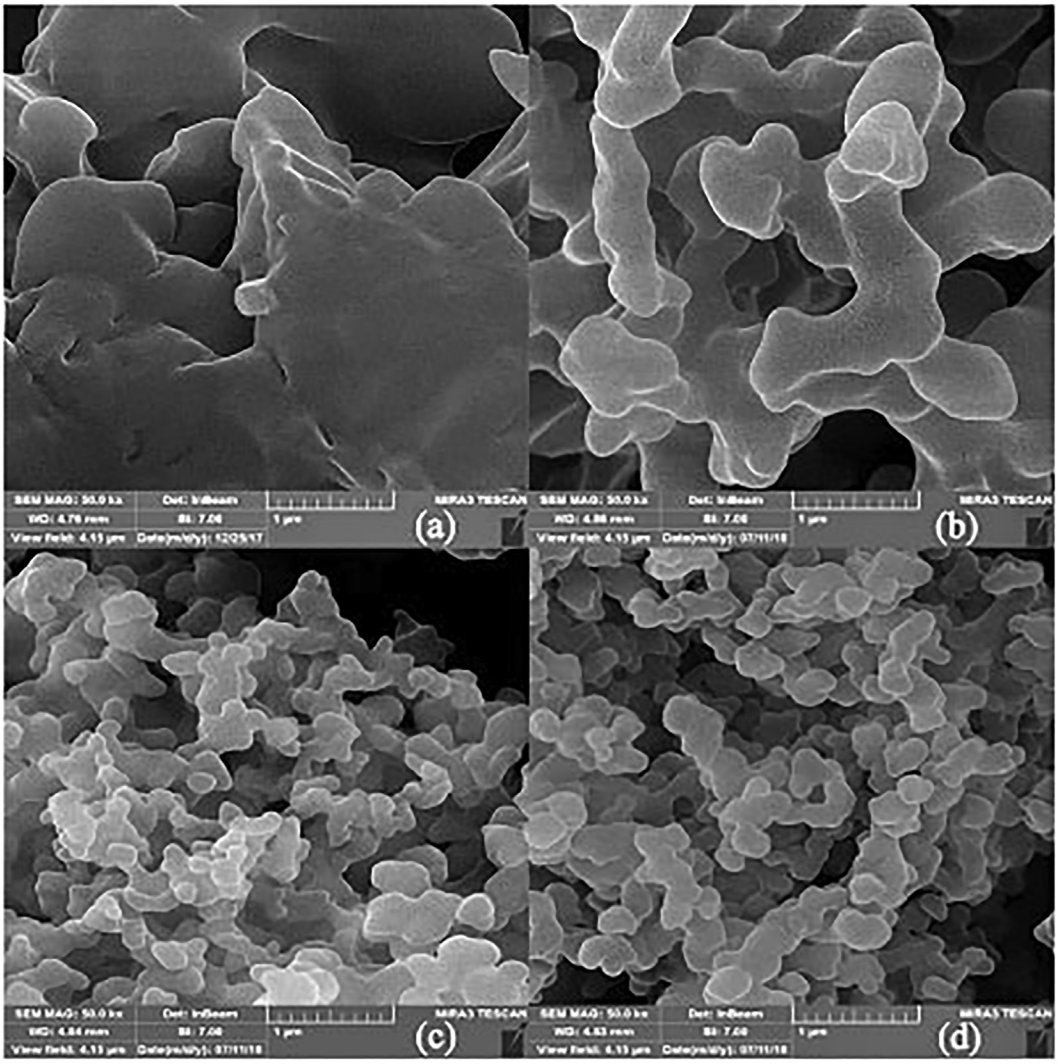

Fig. 5 The FE-SEM images of P(GMA-alt-MA) (a), Sample A (b), Sample B (c) and Sample C (d). All the images with the same magnification (50.0 kx).

3. Results and discussion

The synthesis process of PG-a-M was carried out via thermally initiated free radical polymerization (FRP) of the GMA and the MA in an equal molar ratio in the presence of the AIBN as the free radical generator (Scheme 1). This copolymer (as an alternative copolymer consists of two active functional groups (epoxy and anhydride) on each repeating unit (Hasanzadeh et al., 2016). Therefore, it is a suitable choice for the modification and preparation of drug carriers.

The modification of the prepared P(GMA-alt-MA) was implemented by the reaction of the IPA as the modifying agent and the EDA as the crosslinking agent (Scheme 2) with different molar ratios. Addition of IPA to copolymer was done to create amidic or amine groups along with carboxylic acid groups in copolymer backbone to become the pH responsive hydrogel. The prepared hydrogel with basic and acidic functional groups can acts as stimuli-responsive materials, which can undergo sudden volume changes in response to small changes in their environmental factors including the pH and temperature.

Also it is obvious that by increasing the ratio of the crosslinking agent, the cavities in hydrogel network become smaller and the rigidity of the final product increases and resists against higher swelling; thus it effects on the loading capacity of the sample and subsequently the amount of the released drug. These parameters are discussed in the following sections.

3.1. Structural characterization

3.1.1. FT-IR

Fig. 2 shows the FT-IR spectra of the samples. In Fig. 2-a which is related to the P(GMA-alt-MA), the absorption bonds at 1783 and 1856 cm^{-1} are attributed to the carbonyl groups (C═O) of the MA. Also the peaks at 1730 and 1073 cm^{-1} are related to the stretching vibrations of C═O and C─O, respectively, indicating the presence of ester groups. Moreover, the absorption bond at 911 cm^{-1} is assigned to the epoxide groups.

The FT-IR spectrum of the amino-modified P(GMA-alt-MA) is shown in Fig. 2-b. As shown in this figure, the stretch-

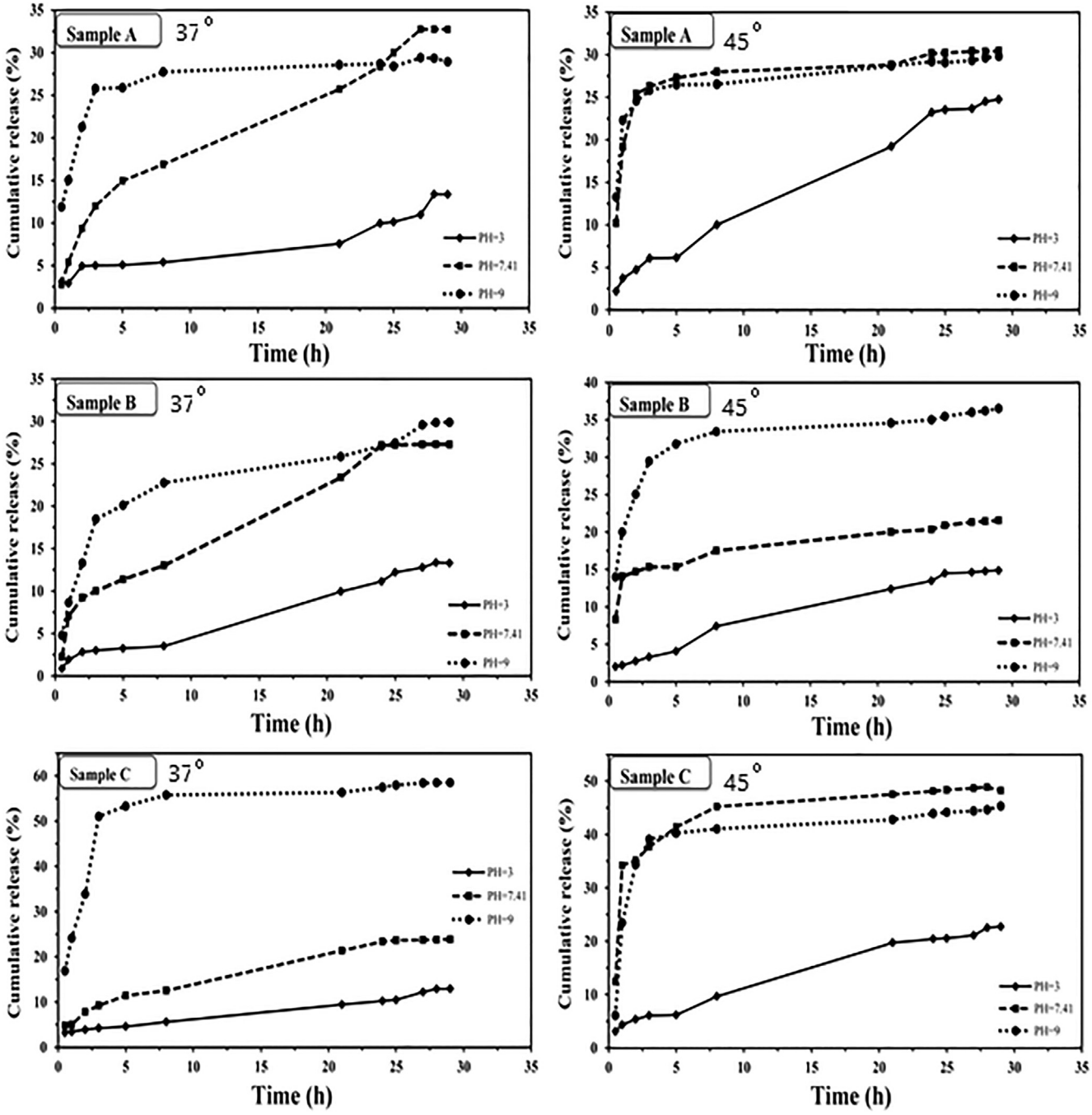

Fig. 6 The release profiles of FR from the samples.

ing vibrations of the amidic carbonyl groups are appeared at 1648 cm^{-1}, indicating the successful modification reaction. Besides, the esteric carbonyls of the P(GMA-alt-MA) units are still remaining at 1734 cm^{-1} indicating that the modifying agent did not attack to the esteric carbonyls. An obvious shoulder is observed on the right side of this peak, which is attributed to the carboxylic acids generated from ring opening of the anhydride groups by the attack of amines. Moreover, the bending vibrations of the N—H bonds are shown at 1462 cm^{-1} and the broad peak between 3200 and 3500 cm^{-1} corresponds to the stretching vibrations of N—H and O—H bonds. Furthermore, the stretching vibrations of free N—H and free O—H bonds are shown at 3742 and 3852 cm^{-1}, respectively. Also the C—H stretching vibrations can be observed at 2930 cm^{-1}.

3.1.2. Structural characterization of the GMA-MA copolymer by ^1H NMR spectrum

The ^1H NMR spectrum of the prepared GMA-MA copolymer was shown in Fig. 3. The methyl groups of GMA moieties are appeared at 0.97, 1.16 ppm due to different steric effects (Hasanzadeh et al., 2016). The peak related to CH_2 in the main

chain was presented at 1.97 ppm. The anhydride CH groups were appeared at 2–2.20 ppm. Three peaks, belonging to the epoxy groups were appeared in the range of 2.64–3.49 ppm. The proton of the chiral carbon on the epoxy ring resonates at 3.3 ppm whereas diasrotopic protons of epoxy ring (—CH2—) resonate between 2.6 and 2.9 ppm. Diastrotopic protons on —O— CH_2— of the ester groups resonate at the range of 3.71–4.42 ppm.

3.1.3. Thermal gravimetric analysis (TGA)

To describe the behavior of a sample as a function of temperature, thermal gravimetric analysis (TGA) is used to demonstrate degradation processes and thermal stability studies (Hatakeyama and Quinn, 1999). Fig. 4 shows the TGA thermograms of the P(GMA-alt-MA) and the sample A. A slight weight loss can be seen in the curve of the sample A up to 100 °C; which is due to the evaporation of the moisture in sample. In the thermogram of P(GMA-alt-MA), a sharp degradation step is observable between 320 and 470 °C which is attributed to the decomposition of the bare P(GMA-alt-MA) chains. As shown in the thermogram of the sample A, the main degradation point started from lower temperature than that of the bare copolymer (230 °C), and the degradation range has been broadened. This is due to the degradation of the pendant IPA groups in the first step (up to 400 °C) and then the crosslinked chains degradation in the second step (up to 600 °C), respectively.

3.1.4. Field emission scanning electron microscopy (FE-SEM)

In order to investigate and compare the surface morphology of the synthesized hydrogels, FE-SEM technique was employed. Fig. 5 shows the FE-SEM images of samples P(GMA-alt-MA) (a); Sample A (b); Sample B (c) and Sample C (d). The porosity of the samples increased from A to D, with increasing the crosslinker agent ratio in feed of modification reaction and the diameter of the cavities is reduced. This transformation indicates that the modification of P(GMA-alt-MA) copolymer was done successfully. It can be said that, the morphological structures of the hydrogels have an effect on the swelling behavior and subsequently on the drug loading and releasing behavior.

3.2. Swelling studies

The most important consideration in hydrogels is to determine their swelling, which plays a significant role as drug carriers used in controlled release. The ESR was calculated for the samples A, B and C and the obtained data were 9.5, 7.6 and 6.8, respectively. It is well known that the swelling of hydrogel is induced by the porosity and electrostatic repulsion of the

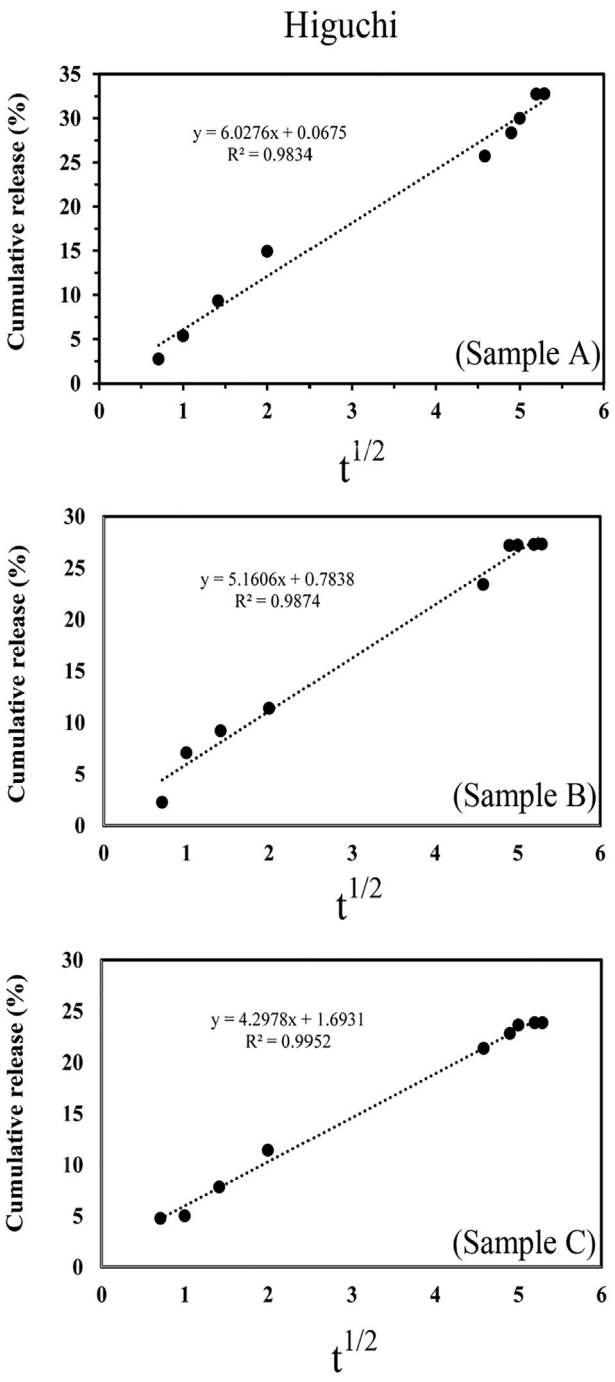

Fig. 7 The plot of the best kinetic model (higuchi) for each of the samples, Sample A, Sample B and Sample C.

Table 1 Mathematical models used to study the release kinetics.

Model	Mathematical equation	Y axis	X axis	Slope	y intercept	Original references
Zero order	$Q_t - Q_0 = k_0 t$	Q_t	T	k_0	Q_0	(Lokhandwala et al., 2013)
First order	$LogQ_t - LogQ_0 = k_0 t/2.303$	$LogQ_t$	t	$k_0/2.303$	$LogQ_0$	(Costa and Lobo, 2001)
Korsmeyer–Peppas	$M_t/M_\infty = kt^n$	Log (M_t/M_∞)	Log t	n	nLogk	(Korsmeyer et al., 1983)
Higuchi	$Q_t = k_H t^{1/2}$	Q_t	$t^{1/2}$	k_H	0	(Higuchi, 1961)
Hixson-Crowell	$Q_0^{1/3} - Q_t^{1/3} = kt$	$Q_0^{1/3} - Q_t^{1/3}$	T	k	0	(Hixson, and Crowell, 1931)

ionic charges in hydrogel network (Karadag et al., 2002). The porosity and rigidity of hydrogel network are influenced by density of crosslinker so, the swelling behavior in the synthesized hydrogel of this work by changing crosslinker density can be interpreted thought the fact that, more the ratio of EDA is increased, the swelling of the hydrogels is more reduced; because the hydrogel becomes more compact form and less space is created for water penetration.

3.3. Drug loading and in vitro release studies

The loading process of drug on synthesized hydrogel was carried out by immersion procedure in high concentration of the drug solution via propagation and penetration process. The loading capacity percentage for the samples A, B and C is 18.18, 9.51 and 8.76, respectively. According to the LC% amounts, the sample A has the highest LC%. So, it can be predicted that the formed cavities in this hydrogel network have good proportional with the diameter of the FR molecules and effective interaction between them have been formed respect to the other synthesized hydrogel (Fig. 5). On the other hand, by increasing the EDA ratio, the cavities become smaller in the result of increasing of crosslinker density in the hydrogel network and the LC% decreases; therefore, the amount of the released drug decreases subsequently. However, in overall the good percentage of the loading capacity is due to the high chain length of a polymeric chains and the presence of the proper functional groups which have a good interaction with the drug functional groups. The release of the FR from the bed of synthesized carriers in PBS buffer was investigated in three different pH values of 3 and 7.4 and 9. Also, for investigation of probable thermal sensitive properties of the synthesized carriers the drug release studies were carried out in two different temperatures. The results were summarized as a plots in Fig. 6. As shown in Fig. 6, all the samples have shown pH dependent properties and the maximum release rate was shown in basic pH. The reason for this faster release in higher pH is related to the decrease of absorption between drug and carrier caused by the deprotonation of the electronegative groups in the nanoparticles composition, which leads to the carrier negative filaments expands and also some of the hydrogen bonds are broken and the FR enters the environment more rapidly. Also negative repulsion between negative groups of the drug and carriers is occurred in basic medium. In a neutral environment, the hydrogen bonds between the nanoparticles and the drug are important so, the release rate of the drug became slower. However, in acidic medium all the active sites are in the protonated form so, the hydrogen bonding between drug and functional groups of carriers are more important.

The results of drug release in different temperatures showed almost thermal sensitivity properties for synthesized carriers and release rate become faster by increasing the medium temperature. In fact, in higher temperature the rate of propagation and penetration become faster.

3.4. The study of release kinetics

To study the release kinetics, different models were plotted for all of the samples and the several mathematical models were used for this purpose. The used mathematical models were listed in Table 1. The comparison of the square coefficient correlation (R^2) values showed the best fit with the Higuchi model for all samples in this study. Based on this model, percentages of cumulative release verses square root of time were plotted and the results were shown in Fig. 7. The Higuchi model can be used to describe the drug release from matrix systems. Also, by using the Korsmeyer-Peppas model, the values of the diffusion exponent parameter (n) were obtained. In this model, the drug release mechanism is determined based on the n values. The values of $n \leq 0.43$ shows a Fickian diffusion mechanism, $0.43 < n < 0.85$ shows a non Fickian transport, $n = 0.85$ indicates the zero-order release (case II transport) kinetics, and $n > 0.85$ indicates the super case II transport (Ritger and Peppas, 1987). Based on the n values obtained, the drug release follows from the Fickian diffusion in the sample including 30% crosslinking agent. This means that the drug release mechanism is mainly through the diffusion (Fu and Kao, 2010). In the samples containing 10% and 20% crosslinking agent, the drug release follows from the non-Fickian transport. This implies that the drug release mechanism is not just through the diffusion (Fu and Kao, 2010). In the two latter cases, the polymer erosion can occur due to the less amounts of crosslinking agent and the less rigidity, which causes the drug release is carried out through the polymer erosion in addition to the diffusion. The results were shown in table 2.

Table 2 The kinetic parameters of the best-fitted model for each of the samples.

Parameter*	Sample		
	A	B	C
R^2 (Zero order)	0.9611	0.9645	0.9726
R^2 (First order)	0.8103	0.7812	0.9032
R^2 (Korsmeyer–Peppas)	0.9691	0.9366	0.9896
R^2 (Hixson-Crowell)	0.9611	0.9645	0.9726
R^2 (Higuchi)	0.9834	0.9874	0.9952
N	0.55	0.52	0.43
Release mechanism	non – fickian diffusion	non – fickian diffusion	fickian diffusion
k_H (mg/ $hr^{1/2}cm^2$)	6.0276	5.1606	4.2978

* R^2, n, and k_H are square correlation coefficient; diffusional exponent obtained from Korsmeyer–Peppas model, and rate constant related to Higuchi model, respectively.

4. Conclusion

In this work, poly (glycidyl methacrylate-*alt*-maleic anhydride) P(GMA-alt-MA) was synthesized and modified with IPA and EDA with different molar ratios to prepare drug carriers. These carriers were used to study the in vitro Furosemide slow release as a model drug in a simulated human body medium in terms of pH and temperature. According to the obtained results, different ratios of the crosslinking agent (EDA) do not effect on the release rates; but affects the amount of the released drug. Therefore, the sample with the lowest ratio of the EDA was chosen as the best carrier. Also the obtained results showed that all the samples have shown pH dependent properties and the maximum release rate was shown in basic pH. The results of drug release in different temperatures showed almost thermal sensitivity properties for synthesized carriers and release rate become faster by increasing the medium temperature. Moreover, the release kinetics was also investigated using different mathematical models and the Higuchi model had the most adaption with the release data. The results showed that release mechanism in the sample C follows from the Fickian diffusion and the other samples from non-Fickian transport.

Declaration of Competing Interest

There is no conflict of interest for declare.

Acknowledgements

The authors wish to acknowledge the financial and spiritual supports from the Urmia University.

References

Ahmed, E.M., 2015. Hydrogel: preparation, characterization, and applications: a review. J. Adv. Res. 6 (2), 105–121.

Bierbrauer, F., 2005. Hydrogel drug delivery: diffusion models.

Cartmell, J.V., Sturtevant, W.R., Bausmith III, W.E., Wolf, M.L., 1996. Transparent hydrogel wound dressing with release tab. In: Google Patents.

Chen, J., Blevins, W.E., Park, H., Park, K., 2000. Gastric retention properties of superporous hydrogel composites. J. Control. Release 64 (1-3), 39–51.

Cheng, H.W.B., Sham, M.-K., Chan, K.-Y., Li, C.-W., Au, H.-Y., Yip, T., 2014. Combination therapy with low-dose metolazone and furosemide: a "needleless" approach in managing refractory fluid overload in elderly renal failure patients under palliative care. Int. Urol. Nephrol. 46 (9), 1809–1813.

Ciolino, J.B., Hoare, T.R., Kohane, D.S., 2013. Contact lens drug delivery device. In: Google Patents.

Costa, P., Sousa Lobo, J.M., 2001. Modeling and comparison of dissolution profiles. Eur. J. Pharm. Sci. 13 (2), 123–133.

Darandale, S.S., Vavia, P.R., 2012. Design of a gastroretentive mucoadhesive dosage form of furosemide for controlled release. Acta Pharm. Sinica B 2 (5), 509–517.

Das, M., Senapati, P., 2008. Furosemide-loaded alginate microspheres prepared by ionic cross-linking technique: Morphology and release characteristics. Indian J. Pharm. Sci. 70 (1), 77–84. https://doi.org/10.4103/0250-474X.40336.

Franz, C.C., Hildbrand, C., Born, C., Egger, S., Ratz Bravo, A.E., Krahenbuhl, S., 2013. Dose adjustment in patients with liver cirrhosis: impact on adverse drug reactions and hospitalizations. Eur. J. Clin. Pharmacol. 69 (8), 1565–1573.

Fu, Y., Kao, W.J., 2010. Drug release kinetics and transport mechanisms of non-degradable and degradable polymeric delivery systems. Expert Opinion Drug Delivery 7 (4), 429–444.

Hasanzadeh, R., Moghadam, P.N., Bahri-Laleh, N., Ziaee, F., 2016. A reactive copolymer based on Glycidylmethacrylate and Maleic Anhydride: 1-synthesis, characterization and monomer reactivity ratios. J. Polym. Res. 23 (8), 150. https://doi.org/10.1007/s10965-016-1048-8.

Hatakeyama, T., Quinn, F., 1999. Thermal analysis: fundamentals and applications to polymer science. Chichester, New York.

Hoare, T.R., Kohane, D.S., 2008. Hydrogels in drug delivery: Progress and challenges. Polymer 49 (8), 1993–2007.

Higuchi, T., 1961. Rate of release of medicaments from ointment bases containing drugs in suspension. J. Pharm. Sci. 50 (10), 874–875.

Hixson, A.W., Crowell, J.H., 1931. Dependence of reaction velocity upon surface and agitation. Ind. Eng. Chem. 23 (8), 923–931.

Karadag, E., Uzum, O.B., Saraydin, D., 2002. Swelling equilibria and dye adsorption studies of chemically crosslinked superabsorbent acrylamide/maleic acid hydrogels. Eur. Polym. J. 38 (11), 2133–2141.

Kashyap, N., Kumar, N., Kumar, M.N.V.R., 2005. Hydrogels for pharmaceutical and biomedical applications. Crit. Rev. Ther. Drug Carrier Syst. 22 (2), 107–150.

Korsmeyer, R.W., Gurny, R., Doelker, E., Buri, P., Peppas, N.A., 1983. Mechanisms of solute release from porous hydrophilic polymers. Int. J. Pharm. 15 (1), 25–35.

Lee, K.Y., Mooney, D.J., 2001. Hydrogels for tissue engineering. Chem. Rev. 101 (7), 1869–1880.

Limmer, F., Schinner, E., Castrop, H., Vitzthum, H., Hofmann, F., Schlossmann, J., 2015. Regulation of the Na + -K + -2Cl − cotransporter by cGMP/cGMP-dependent protein kinase I after furosemide administration. FEBS J. 282 (19), 3786–3798.

Lin, B.M., Curhan, S.G., Wang, M., Eavey, R., Stankovic, K.M., Curhan, G.C., 2016. Hypertension, diuretic use, and risk of hearing loss. Am. J. Med. 129 (4), 416–422.

Lokhandwala, H., Deshpande, A., Deshpande, S., 2013. Kinetic modeling and dissolution profiles comparison: an overview. Int. J. Pharm. Bio. Sci. 4 (1), 728–773.

Maia, J., Ribeiro, M.P., Ventura, C., Carvalho, R.A., Correia, I.J., Gil, M.H., 2009. Ocular injectable formulation assessment for oxidized dextran-based hydrogels. Acta Biomater. 5 (6), 1948–1955.

Mano, J., Reis, R., Cunha, A., 2002. Dynamic mechanical analysis in polymers for medical applications. In: Polymer Based Systems on Tissue Engineering, Replacement and Regeneration. Springer, pp. 139–164.

Muzammil, E., Khan, A., Stuparu, M.C., 2017. Post-polymerization modification reactions of poly(glycidyl methacrylate)s. RSC Adv. 7 (88), 55874–55884.

Omidian, H., Rocca, J.G., Park, K., 2005. Advances in superporous hydrogels. J. Control. Release 102 (1), 3–12.

Osvath, Z., Toth, T., Ivan, B., 2017. Synthesis, characterization, LCST-type behavior and unprecedented heating-cooling hysteresis of poly(N-isopropylacrylamide-co-3-(trimethoxysilyl) propyl methacrylate) copolymers. Polymer 108, 395–399.

Owen, D.R.J., MacAllister, R., Sofat, R., 2015. Intravenous furosemide for acute decompensated congestive heart failure: what is the evidence?. Clin. Pharmacol. Ther. 98 (2), 119–121.

Pourzitaki, C., Tsaousi, G., Manthou, M.E., Karakiulakis, G., Kouvelas, D., Papakonstantinou, E., 2016. Furosemide modifies heart hypertrophy and glycosaminoglycan myocardium content in a rat model of neurogenic hypertension. Eur. J. Pharmacol. 784, 155–163.

Ritger, P.L., Peppas, N.A., 1987. A simple equation for description of solute release II. Fickian and anomalous release from swellable devices. J. Control. Release 5 (1), 37–42.

Shohraty, F., Moghadam, P.N., Fareghi, A.R., Movagharnezhad, N., Khalafy, J., 2018. Synthesis and characterization of new pH-sensitive hydrogels based on poly(glycidyl methacrylate-co-maleic anhydride): research article. Adv. Polym. Technol. 37 (1), 120–125.

Sinirlioglu, D., Muftuoglu, A.E., Bozkurt, A., 2015. Investigation of perfluorinated proton exchange membranes prepared via a facile strategy of chemically combining poly (vinylphosphonic acid) with PVDF by means of poly (glycidyl methacrylate) grafts. J. Polym. Res. 22, 154–171. https://doi.org/10.1007/s10965-015-0796-1.

Trachtova, S., Zapletalova, H., Spanova, A., Horak, D., Kolarova, H., Rittich, B., 2015. The evaluation of magnetic polymethacrylate-based microspheres used for solid phase DNA micro-extraction. Chromatography 2 (2), 156–166. https://doi.org/10.3390/chromatography2020156.

Vashist, A., Vashist, A., Gupta, Y.K., Ahmad, S., 2014. Recent advances in hydrogel based drug delivery systems for the human body. J. Mater. Chem. B 2 (2), 147–166.

Vigil-De Gracia, P., Dominguez, L., Solis, A., 2014. Management of chronic hypertension during pregnancy with furosemide, amlodipine or aspirin: a pilot clinical trial. J. Mater.-Fetal Neonatal Med. 27 (13), 1291–1294.

Wichterle, O., LIM, D., 1960. Hydrophilic gels for biological use. Nature 185 (4706), 117–118 https://doi/10.1038/185117a0.

Zhuo, R.X., Wei, H., Cheng, C., Chang, C., Chen, W.Q., Cheng, S.X., Zhang, X.Z., 2008. Synthesis and applications of shell cross-linked thermoresponsive hybrid micelles based on poly (N-isopropylacrylamide-co-3-(trimethoxysilyl) propyl methacrylate)-b-poly (methyl methacrylate). Langmuir 24 (9), 4564–4570. https://doi.org/10.1021/la703320h.